**Atmospheric
Chemistry
and Physics**

Airborne measurement of OH reactivity during INTEX-B

J. Mao[1,*], **X. Ren**[1,**], **W. H. Brune**[1], **J. R. Olson**[2], **J. H. Crawford**[2], **A. Fried**[3], **L. G. Huey**[4], **R. C. Cohen**[5], **B. Heikes**[6], **H. B. Singh**[7], **D. R. Blake**[8], **G. W. Sachse**[9], **G. S. Diskin**[9], **S. R. Hall**[10], and **R. E. Shetter**[10]

[1]Department of Meteorology, Pennsylvania State University, University Park, PA, USA

[2]Science Directorate, NASA Langley Research Center, Hampton, VA, USA

[3]Earth Observing Laboratory, National Center for Atmospheric Research, Boulder, CO, USA

[4]School of Earth and Atmospheric Sciences, Georgia Institute of Technology, Atlanta, GA, USA

[5]Department of Chemistry and Department of Earth and Planetary Science, University of California Berkeley, Berkeley, CA, USA

[6]Graduate School of Oceanography, University of Rhode Island, Narragansett, RI, USA

[7]NASA Ames Research Center, Moffett Field, CA, USA

[8]Department of Chemistry, University of California, Irvine, CA, USA

[9]Science Directorate, NASA Langley Research Center, Hampton, VA, USA

[10]Atmospheric Chemistry Division, National Center for Atmospheric Research, Boulder, CO, USA

[*]now at: School of Engineering and Applied Sciences, Harvard University, Cambridge, MA, USA

[**]now at: Rosenstiel School of Marine and Atmospheric Science, University of Miami, Miami, FL, USA

Abstract. The measurement of OH reactivity, the inverse of the OH lifetime, provides a powerful tool to investigate atmospheric photochemistry. A new airborne OH reactivity instrument was designed and deployed for the first time on the NASA DC-8 aircraft during the second phase of Intercontinental Chemical Transport Experiment-B (INTEX-B) campaign, which was focused on the Asian pollution outflow over Pacific Ocean and was based in Hawaii and Alaska. The OH reactivity was measured by adding OH, generated by photolyzing water vapor with 185 nm UV light in a moveable wand, to the flow of ambient air in a flow tube and measuring the OH signal with laser induced fluorescence. As the wand was pulled back away from the OH detector, the OH signal decay was recorded; the slope of $-\Delta\ln(\text{signal})/\Delta$ time was the OH reactivity. The overall absolute uncertainty at the 2σ confidence levels is about $1\,\text{s}^{-1}$ at low altitudes (for decay about $6\,\text{s}^{-1}$), and $0.7\,\text{s}^{-1}$ at high altitudes (for decay about $2\,\text{s}^{-1}$). From the median vertical profile obtained in the second phase of INTEX-B, the measured OH reactivity ($4.0\pm1.0\,\text{s}^{-1}$) is higher than the OH reactiv-

ity calculated from assuming that OH was in steady state ($3.3\pm0.8\,\text{s}^{-1}$), and even higher than the OH reactivity that was calculated from the total measurements of all OH reactants ($1.6\pm0.4\,\text{s}^{-1}$). Model calculations show that the missing OH reactivity is consistent with the over-predicted OH and under-predicted HCHO in the boundary layer and lower troposphere. The over-predicted OH and under-predicted HCHO suggest that the missing OH sinks are most likely related to some highly reactive VOCs that have HCHO as an oxidation product.

1 Introduction

The hydroxyl radical (OH) and the hydroperoxyl radical (HO_2), collectively called HO_x, are central players in atmospheric chemistry. OH acts as the most important oxidizer and cleansing agent in the atmosphere on local to global scales. Its close chemical relative, HO_2, is a major precursor of tropospheric ozone in the presence of NO_x. HO_x initiates and participates in almost all of the complex chemical pathways in the atmosphere. OH levels are dependent on atmospheric constituents emitted by biogenic and anthropogenic processes. To test the understanding of atmospheric OH, OH

measurements are typically compared to OH calculated by models that are constrained by simultaneous measurements of other atmospheric constituents. When measured and modeled OH disagree, the completeness of the measurement suite often comes into question.

The completeness of the measurement suite can be tested directly for atmospheric constituents that react with OH by measuring the OH reactivity, the inverse of the OH lifetime. The OH reactivity is the sum of the products of the concentrations and their reaction rate coefficients for all gases that react with OH. It is defined as:

$$k_{OH} = \sum k_{OH+VOC_i} [VOC_i] + k_{OH+CO} [CO] + k_{OH+NO} [NO] + k_{OH+NO_2} [NO_2] + k_{OH+SO_2} [SO_2] + \ldots\ldots \quad (1)$$

Kovacs and Brune (2001) designed the first version OH reactivity instrument with the flow tube technique and successfully measured the ambient OH reactivity for the first time on the ground. This first version of OH reactivity instrument was also deployed in several other ground campaigns (Kovacs et al., 2003; Ren et al., 2003, 2004, 2006; Di Carlo et al., 2004; Shirley et al., 2006). The flash photolysis technique was developed by Jeanneret et al. (2001) and Sadanaga et al. (2004) for measuring the ambient OH reactivity. Sadanaga et al. (2005) successfully made field measurements in an urban area. These studies have demonstrated general agreement between measured and calculated OH reactivity for some urban environments and a surprising temperature dependent missing OH reactivity in forests (Di Carlo et al., 2004). More recently Sinha et al. (2008) developed a new method to measure OH reactivity by monitoring the change of OH reactants within the range of OH reactivity at $6\sim300\,s^{-1}$. Moreover, the OH reactivity measurements have proved valuable for examining OH sources using the assumption of the balance between OH production and loss.

This paper presents a new airborne version of the Penn State OH reactivity instrument and the first airborne measurements of OH reactivity. The measurements were made during the NASA Intercontinental Chemical Transport Experiment – B (INTEX-B) mission in April/May 2006. The analysis includes comparisons of the measured OH reactivity with OH reactivity calculated by two independent methods as discussed later.

2 Instrumentation

The OH reactivity, k_{OH}, can be directly acquired by measuring OH decay rate as follows

$$\frac{d[OH]}{dt} = -k_{OH}[OH] \quad (2)$$

If the reactant concentrations change little when exposed to OH, the OH decay rate is assumed to be pseudo-first order

(reactants remain constant). Assuming k_{OH} is constant during the decay, the OH reactivity can be determined from the equation:

$$k_{OH} = -\frac{\ln \frac{[OH]}{[OH]_0}}{\Delta t} \quad (3)$$

where $[OH]_0$ represents the initial OH concentration, and $[OH]$ represents the OH concentrations after a reaction time Δt between OH and its reactants.

The OH reactivity is measured by adding OH, which is generated by photolyzing water vapor with 185 nm ultraviolet light in a moveable wand, to the flow of ambient air and measuring the OH signal with laser induced fluorescence. The aluminum flow tube is 7.5 cm in diameter and 40 cm long between the inlet and the aluminum block that attaches to the OH detection system (Fig. 1a). The movable wand, which is 2.0 cm in diameter, is attached through a slot in the flow tube to a lead screw, which is turned by a stepper motor. As the wand is pulled back, the OH signal decay is recorded; the slope of $-\frac{\ln \frac{[OH]}{[OH]_0}}{\Delta t}$ is the OH reactivity. Nine steps of 1.0 cm are used for each complete decay. The air flow velocity is approximately $0.5\,m\,s^{-1}$, so that each step is equivalent to Δt=0.02 s. The wand stays at each step for 20 s before moving in less than 0.5 s to the next step. Measuring the whole decay takes about 3.5 min. A sample decay obtained on the flight of 23 April 2006 shows the nine steps and the good linearity over three decay lifetimes (Fig. 1b). The linear regression algorithm is based on unweighted linear squares fitting and improved to remove the outliers in the decay, which could be due to the fast changing air mass the aircraft encountered within each single decay of 3.5 min. The collected OH reactivity data shows very few decays were affected by the fast changing air mass during flight.

The OH signal is detected by Laser Induced Fluorescence (LIF) in a low pressure chamber (Faloona et al., 2004). OH is excited and emits fluorescence by the following process:

$$X^2\Pi(v''=0) \to A^2\Sigma^+(v'=0) \to X^2\Pi(v''=0) \quad (4)$$
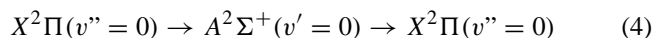
where $X^2\Pi(v''=0)$ is the ground state of OH, and $A^2\Sigma^+(v'=0)$ is the excited state. After absorbing laser light with a wavelength around 308 nm, the excited OH transits to the ground state spontaneously and emits fluorescence in the wavelength range from 307 nm to 311 nm simultaneously. The laser consists of a dye laser that is pumped by a diode-pumped Nd:YAG laser (Spectra-Physics, X30SC-1060A) at 3 kHz pulse frequency. The output of this dye laser is 308 nm UV light. Adjustment of laser wavelength can be achieved by an etalon.

The etalon is tuned on-line with OH fluorescence for 15 s and then off-line for 5 s to measure the background. The difference in the average on-line and average off-line signals is the OH fluorescence. The OH fluorescence is proportional to the OH mixing ratio. Because of this proportionality, the
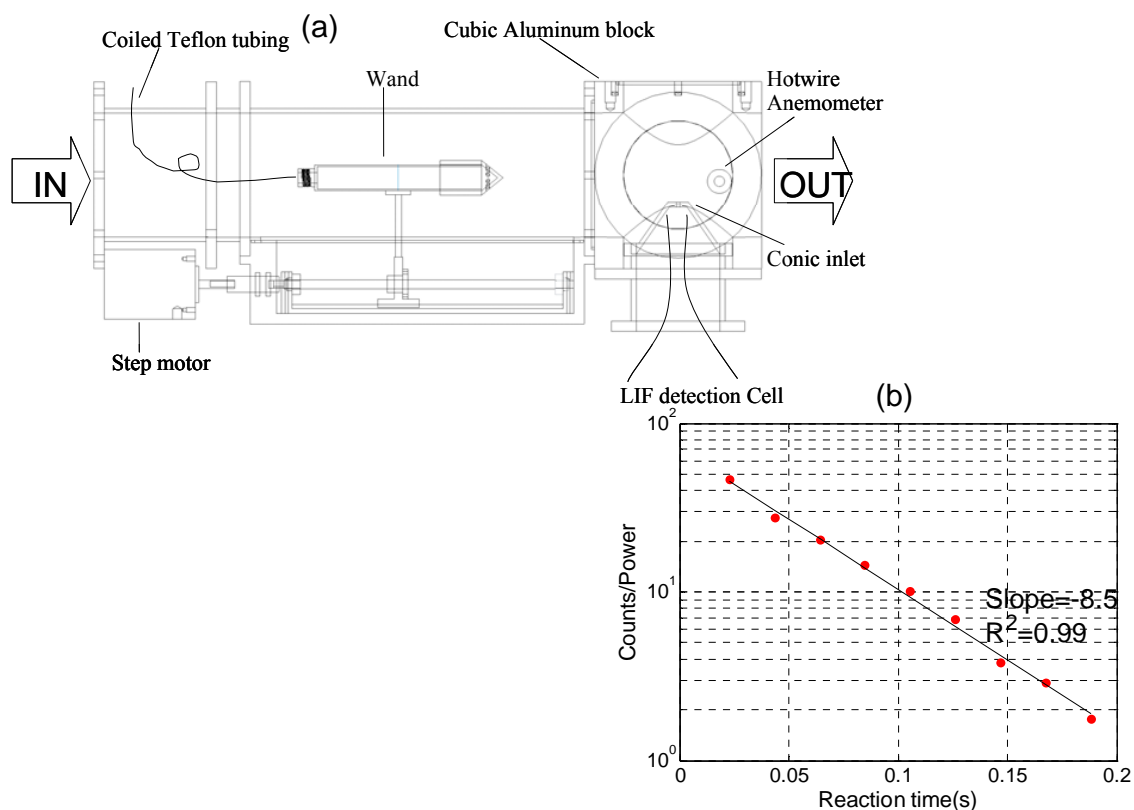
Fig. 1. Schematic diagram (a) and sample decay (b) of the OH reactivity instrument. In the schematic diagram **(a)**, the left part is the aluminum flow tube with the linear transmission system sitting below the tube. The right part is the cubic aluminum block with conic inlet for OH detection. The sample air flows in from the left side of the flow tube, reacts with the OH injected out from the wand, and flows out from the right side of the cubic aluminum block. The sample decay **(b)** was obtained on the 23 April 2006 flight when flying through the boundary layer. In this case, the measured OH reactivity is about $6.5\,s^{-1}$ ($8.5\,s^{-1}$ minus wall loss of $2.0\,s^{-1}$).

OH reactivity measurement does not require knowledge of the OH concentrations, although the OH detection system is calibrated and indicates typical OH and HO_2 concentration is about 100pptv in the flow tube.

The air sample is pulled into the vacuum detection system (from 3~12 hPa) through an orifice on a conical inlet (orifice ID is about 0.56 mm). This inlet sits 5 cm downstream of the flow tube. Inside the detection system, the laser beam crosses the detection axis that includes a gated microchannel plate (MCP) detector (Hamamatsu R2024U-06), which is set perpendicular to the airflow and the laser beam to detect the fluorescence emitted by the OH.

The OH reactivity instrument was installed in a rack in the forward cargo bay on the NASA DC-8. The inlet tube (1.5 cm dia.) protruded 10 cm below the aircraft skin. The end of the tube was cut at a 45° angle, facing forward, to create a ram force. This inlet was connected to the OH reactivity instrument with a 1 m long, 2.5 cm diameter stainless steel flexible line. The air flowed through the instrument and down another line that was connected to an exhaust port downstream of the inlet.

The reaction time depends critically on the velocity of the air flow in the tube. The velocity is measured at the center of the flow tube just downstream of the OH detection system inlet with a hotwire anemometer (TSI 8455-03 Air Velocity Transducer). All the in situ velocity measurements from the hotwire anemometer need to be corrected by the ambient pressure and temperature to calculate the actual velocity inside the flow tube. This anemometer comes calibrated only for pressures near 1 atmospheric pressure, while the pressure inside the flow tube, which is equal to the ambient pressure, varied from 200 hPa~1000 hPa. Thus, the anemometer was calibrated for low pressures.

To mimic the flow conditions during flight, the instrument was connected on the ground to a mass flow controller at the upstream end and to a vacuum pump at the downstream end. It was found that the reading of the transducer indicates the standard mass flow and shows no dependence on the pressure (from 20 kPa~100 kPa). Since the reading of the anemometer is a good indicator for the standard mass flow, tests were conducted to investigate the relationship between the anemometer reading and the actual mass flow. The

Table 1. Measurements on NASA DC-8 air plane during INTEX-B.

Chemicals	Methods	Organization
photolysis frequencies	Actinic Flux Spectroradiometer	NCAR
OH, HO$_2$	Laser Induced Fluorescence	Penn State University
H$_2$O	chilled mirror hygrometer	NASA Langley Research Center
NO	Chemiluminescence	Georgia Tech
NO$_2$	Laser Induced Fluorescence	UC-Berkley
O3	Chemiluminescence	NASA Langley Research Center
H$_2$O$_2$,CH$_3$OOH	HPLC-flourometry	University of Rhode Island
CO,CH$_4$	Tunable Diode Laser Absorption Spectrometry	NASA Langley Research Center
HCHO	Tunable Diode Laser Absorption Spectrometry	NCAR
SO$_2$	Chemical Ionization Mass Spectrometry	Georgia Tech
HNO$_3$	Mist chamber/GC-IC	University of New Hampshire
NMHC[a]	Whole air sample collection GC-FID/EC/MS analysis	UC-Irvine
OVOC[b],Nitriles,PANs	GC-ECD/PID/RGD	NASA Ames Research Center

[a] NMHC includes ethane, ethene, propane, propene, i-butane, n-butane, ethyne, i-pentane, npentane, n-hexane, isoprene, benzene, and toluene. [b] OVOC includes acetaldehyde, propanal, acetone, MEK, methanol, and ethanol.

reading of the anemometer at the farthest step of the wand has an excellent linear response to the mass flow.

The temperature increases by more than 30 K as the air speed relative to the aircraft decreases from the ~200 m s^{-1} aircraft speed to less than a few m/s in the flow tube. This "stagnation" temperature increase can be calculated by Eq. (5).

$$V^2 = 2c_p(T - t) \tag{5}$$

where c_p is the specific heat capacity at constant pressure, V is the aircraft velocity, T is the stagnation temperature, and t is the static temperature. If the DC-8 aircraft flies at Mach 0.8, which is about 270 m s^{-1}, c_p is about 1000 J kg^{-1} K^{-1}, the air will be heated up by 37°C when it gets into the OH reactivity instrument flow tube. During the entire INTEX-B study, the lowest temperature inside the flow tube was 270 K when the outside was about 220 K. To calculate the OH reactivity, both the ambient temperature and the temperature inside the flow tube are used, as will be discussed below.

During flight, the flow inside the tube was forced by a combination of ram pressure in the wedge-shaped inlet and the venturi effect on the outlet. An orifice inside the downstream line sets the velocity in the flow tube. The flow tube can be isolated from the atmosphere by two manual butterfly valves (Key High, ISO-KF Interface), which are upstream and downstream of the flow tube respectively.

The flow inside the flow tube was laminar, with the Reynolds number between 200 and 2000 depending on the altitude. However, the laminar parabolic profile was not fully developed. From entrance length theory, the characteristic

length for the development of the parabolic velocity profile is given by l=0.065 d*Re under the laminar flow condition (Gerhart et al., 1992), where d is the diameter of the flow tube and Re is the Reynolds number. The entrance length in the OH reactivity instrument flow tube is estimated to be at least 100 cm, which is twice the length in the flow tube. Therefore, the flow velocity profile was fairly flat in the center and the velocity decreases near the walls. The instrument was frequently calibrated in flight to verify that the air flow in the flow tube is well understood. A mixture of 1% perfluoroethylene (C_3F_6) in air was further diluted in zero air and added to the ambient air upstream of the flow tube. The C_3F_6 reaction rate coefficient used for this calibration is $(6.0\pm0.8)\times10^{-13}$exp[(370$\pm$40)/$T$] cm^3 molecule^{-1} s^{-1} (Dubey et al., 1996). Calibrations were performed at all altitudes, sometimes frequently (Fig. 2a). The median ratio of the measured-to-calculated OH reactivity for C_3F_6 is 1.12$\pm$0.36 and is independent of altitude (Fig. 2b). The increased scatter in the ratio at lower altitudes probably comes from increased variability in the ambient OH reactivity, which must be subtracted from the OH reactivity measured during the calibration to get the measured OH reactivity due to C_3F_6 alone. These calibrations verify that the flows in the OH reactivity instrument are well understood for the entire altitude range of the DC-8.

The OH reactivity instrument was also calibrated in the laboratory. Flight conditions were simulated by controlling the flow of zero air into the instrument with a mass flow controller and by controlling the pressure in the flow tube with a vacuum pump downstream of the
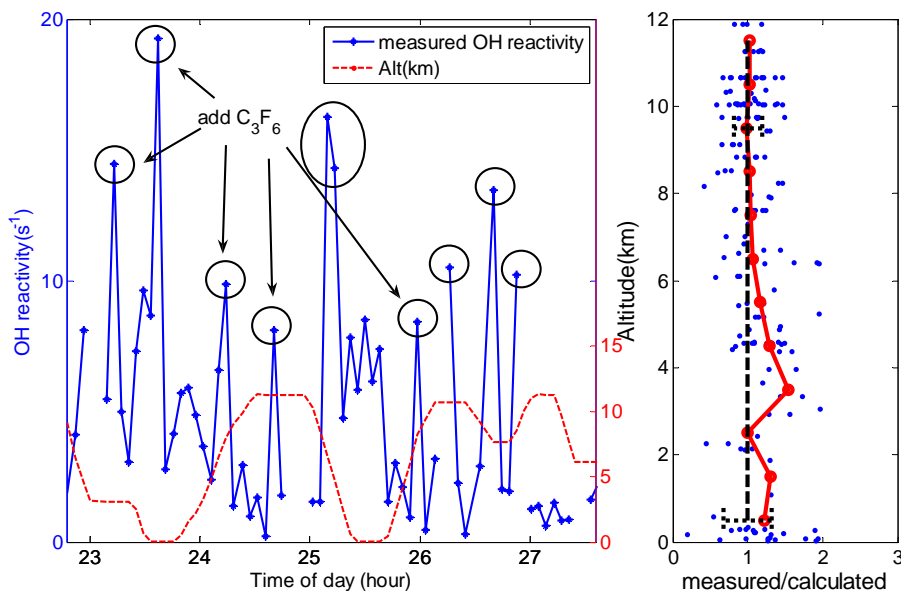
Fig. 2. In situ C_3F_6 calibration on the flight of 23 April 2006 during the INTEX-B field campaign. **(a)** Measured OH reactivity without C_3F_6 added (blue points and lines), with C_3F_6 added (black circled points), and altitude (red dashed line). **(b)**. The ratio of the measured-to-calculated OH reactivity due to C_3F_6 calibrations (blue points) and the median ratio for each kilometer of altitude (red line with points). The dashed line is the one-to-one line and the dotted lines are the 2σ uncertainties.

instrument. Four different calibration gases were added to the zero air upstream of the instrument at three different pressures. The measured OH reactivity was compared to the OH reactivity calculated from the well-known reaction rate coefficients and the known gas concentrations. These calibration gases were 100 ± 5 ppmv carbon monoxide, 10.3 ± 0.5 ppmv propane, 0.92 ± 0.05 ppmv propene (MG Industries), 1.029 ± 0.021 ppmv isoprene (Apel-Riemer Environmental, Inc.). The reaction rate coefficients are from Atkinson et al. (2006) and Sander et al. (2006). The comparison of the measured OH reactivity to the calculated reactivity is excellent for the three pressures (Fig. 3). This test indirectly validates the reaction rate coefficients for CO, isoprene, propane, and propene. Most importantly, it gives confidence in the OH reactivity instrument behavior at different pressures.

In regions where NO levels are greater than a few ppbv, the OH decay can be affected by the reaction of $HO_2+NO\rightarrow OH+NO_2$ inside the flow tube (Kovacs et al., 2003). The observed upward curvature in the decay curve can be corrected if HO_2 decays are also measured and this correction is accurate even with NO is 100 ppbv (Shirley et al., 2006). When NO is 2.5×10^{10} cm^{-3} (1 ppbv at the ground), the calculated decay is about 10% less than the actual decay. However, during the second phase of INTEX-B, the NO was less than 10^9 cm^{-3} for all but a few measurements. As a result, the error in these INTEX-B measurements is at most a few percent.
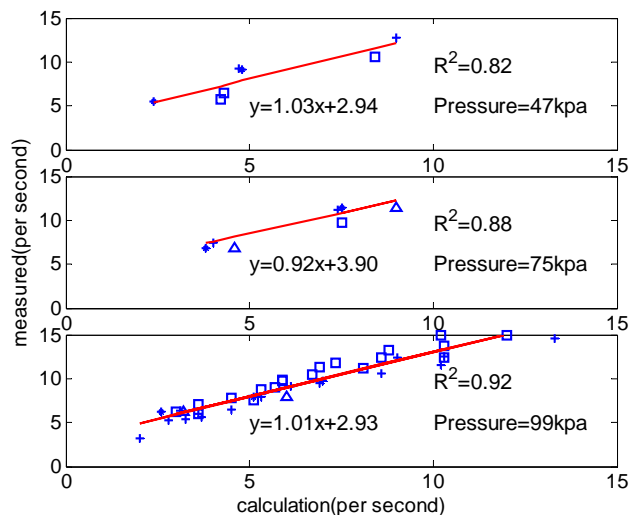

Fig. 3. Laboratory calibration for the OH reactivity instrument using different gases at different pressures. The measured OH reactivity is plotted versus the calculated OH reactivity. Calibration gases include CO (hollow square), isoprene (plus sign), propane (star) and propene (triangle).

The wall loss of OH increases the effective decay of measured OH and must be carefully characterized. It is inevitable that OH gets lost due to wall reactions. Wall loss could be reduced by using Teflon or another coating, but the wall loss could then change in unknown ways with the changes in the
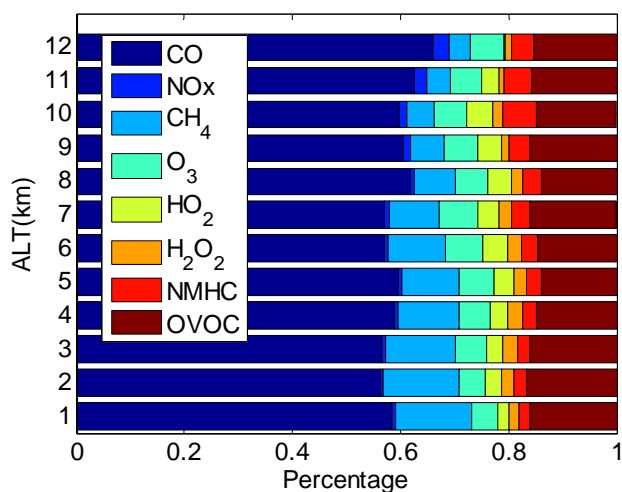
Fig. 4. The median vertical profile of fractional contribution from the main OH losses through the troposphere during the second phase of INTEX-B field campaign. The OH losses include the reactions between OH and its reactants, including CO, NOx, CH4, O3, HO2, H2O2, NMHC, and OVOC.

composition of the sampled ambient air. We prefer to have a steady and slightly larger wall loss that comes with an uncoated metal wall, for which OH is generally lost on each collision with the wall. Thus, the flow tube was not coated with any chemicals to reduce wall loss.

The wall loss must be subtracted from the ambient measurement in order to obtain the measured OH reactivity. Wall loss can be estimated by finding the intercept of linear regression of the measured OH reactivity versus the calculated OH reactivity or by measuring the OH decay in pure air or nitrogen carrier gases. The intercept method gives a median wall loss of $2.9 \pm 0.3 \, \mathrm{s}^{-1}$, while the pure carrier gas method gives an intercept of $2.5 \pm 0.3 \, \mathrm{s}^{-1}$. Both of these methods show that the wall loss is independent of pressure, as is expected by theory (Howard et al., 1979).

However, the wall loss measurement can be affected by trace impurities in the carrier gas for both methods. Thus a third way to find the wall loss is by measuring the OH reactivity in clean ambient air and subtracting the calculated OH reactivity due to measured atmospheric constituents from the measured OH reactivity. Under certain conditions the air at high altitude over Pacific Ocean is clean enough to act as the clean carrier gas and the wall loss is independent of flow tube pressure. The lowest values at high altitudes will be the wall loss. The OH wall loss obtained from ambient measurements is $2.0 \pm 0.3 \, \mathrm{s}^{-1}$. This value is lower than that obtained from the other two methods, suggesting that the pure air and nitrogen do contain some impurities that react with OH. We use the value of $2.0 \pm 0.3 \, \mathrm{s}^{-1}$ as the wall loss.

The uncertainty in the OH reactivity measurement consists of an absolute uncertainty and the uncertainty associated with the wall loss subtraction. The absolute uncertainty of OH reactivity measurement (2σ) mainly depends on following factors: (1) uncertainty of the anemometer, which is 2% of reading from the manufacture specification for Model 8455-03 Air Velocity Transducer and 10% for the temperature and pressure correction; (2) uncertainty of the regression coefficients, which is 15% when the decay is less than $2 \, \mathrm{s}^{-1}$, and 5% when the decay is about $6 \, \mathrm{s}^{-1}$; (3) the statistical precision of the fluorescence signals, which are about $100 \, \mathrm{cts} \, \mathrm{s}^{-1}$ for 15 s at the furthest point, for an uncertainty of 4%; and (4) uncertainty of the measured position of the wand, which is less than 1%. Considering the uncertainty of the wall loss is $0.3 \, \mathrm{s}^{-1}$ throughout the troposphere, the overall absolute uncertainty at the 2σ confidence levels is about $1 \, \mathrm{s}^{-1}$ at low altitudes (for decay about $6 \, \mathrm{s}^{-1}$), and $0.7 \, \mathrm{s}^{-1}$ at high altitudes (for decay about $2 \, \mathrm{s}^{-1}$). The uncertainty in the wall loss sets a minimum for the uncertainty in the measured OH reactivity when the OH reactivity is below $1 \, \mathrm{s}^{-1}$. Thus, the limit of detection for the OH reactivity measurement in INTEX-B was $0.3 \, \mathrm{s}^{-1}$, at the 2σ confidence level.

3 Results

INTEX-B was a NASA project that aimed to understand the intercontinental transport and transformation of chemicals and aerosols and their impacts on air quality and climate (Singh et al., 2009). The platform of INTEX-B included four aircraft: the NASA DC-8, the NSF C-130, the NASA J-31 and the NASA B-200. The Penn State HOx and OH reactivity instruments were installed in the front cargo bay of the NASA DC-8 aircraft. The whole campaign lasted for 10 weeks (from 1 March 2006 to 15 May 2006) and was split into two phases. The first phase was focused on the Mexico City pollution outflow (from 1 March to 21 March, 9 flights) and was based in Houston, TX. The second phase was focused on the Asian pollution outflow (from 23 April to 15 May, 9 flights) and was based in Hawaii and Alaska.

These OH reactivity measurements were the first ever made from on an aircraft. During the first phase of INTEX-B, many adjustments had to be made to the instrument, particularly the air flow in the flow tube. After some tests and modifications, the instrument made measurements successfully in the second phase of the INTEX-B mission. The flight tracks of the second phase of INTEX-B were over the relatively clean Pacific Ocean with some flights over Alaska and the continental United States (Singh et al., 2009). The flight altitude was frequently changed, giving frequent scans over altitudes from 300 m to almost 12 km above the surface. These flight profiles allowed for a significant sampling of OH reactivity over the Pacific Ocean and near the western coast of North America.

3.1 Comparing measured and calculated OH reactivity

The measured OH reactivity is compared to OH reactivity that is calculated using two different methods. The first method is to determine the sum of the products of the measured concentrations of OH reactants and their reaction rate coefficients with OH. The second method is to assume that OH is in steady state; one then calculates the OH production, and finds the OH reactivity that balances the calculated OH production. In this paper, the OH reactivity calculated with the reactants is called "OHRreactants"; and the OH reactivity calculated from OH steady-state is called "OHRrecycling".

The first method to calculate OH reactivity is to sum the products of all OH reactants concentrations and their reaction coefficients with OH, as in Eq. (1). This calculated OH reactivity should agree with the measured OH reactivity if all OH reactants have been measured. Comparing calculated and measured OH reactivity examines the current understanding of OH sinks in the atmosphere.

The measured OH reactants mainly include non-methane hydrocarbons (NMHC), oxygenated volatile organic compounds (OVOC), CO, CH_4, HCHO, NO, NO_2, SO_2, HNO_3, and H_2O_2. NMHC was measured by UC-Irvine and includes 26 alkanes, alkenes, alkynes, aromatics, nitrates, and halogenated compounds. OVOC was mainly measured by NASA Ames Research center and includes acetaldehyde, propanal, methanol, ethanol, acetone, and methyl ethyl ketone (MEK). The large OVOC component formaldehyde was measured by the NCAR tunable diode laser absorption spectrometer (TD-LAS). CO altitude (Fig. 5). The median values are calculated based on all available measurements for each 1km layer from the surface to 12 km.

The $O(^1D)+H_2O$ reaction is a dominant contributor in the lower troposphere, which contributes more than 50% of OH production in the marine boundary layer over the Pacific Ocean. Meanwhile the HO_2+NO reaction dominates the OH production in the upper troposphere, where water vapor mixing ratios are relatively low and NO mixing ratios are relatively high. In addition, the HO_2+O_3 reaction also plays an important role for OH production throughout the whole altitude range.

The measured OH reactivity is compared to the OH reactivity that is calculated with the reactants using the later method (OHRreactants) and the OH reactivity that is calculated from OH steady-state is (OHRrecycling) in Fig. 6. There are periods when the measured and calculated OH reactivity values all agree to within uncertainties, especially at lower values of OH reactivity. However, when the measured OH reactivity exceeds a few s^{-1}, the measured OH reactivity is typically greater than OHRcycling, which is typically greater than OHRreactants. These differences can be quite large (e.g., at day-of-the-year time 135.93 in Fig. 6).

To study the dependence of the measurement with altitude, the median vertical profile (1 km each level) of the measured OH reactivity is plotted against the altitude in Fig. 7. The
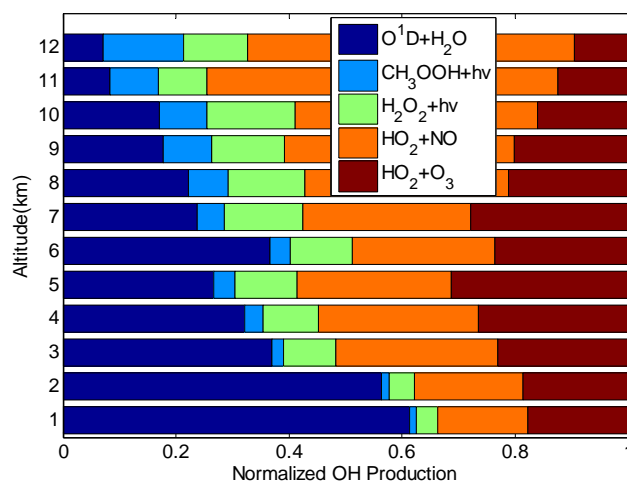

Fig. 5. Fractional contribution of different kinds of OH sources through troposphere in INTEX-B field campaign. OH sources include O $(^1D)+H_2O$, HO_2+NO, HO_2+O_3, the photolysis of CH_3OOH, H_2O_2 and HNO_3.

median values are calculated based on all measured OH reactivity in each 1km layer through the whole troposphere. Medians, interquartile range (25%–75%), and 1.5 times interquartile range (12.5%–87.5%) are all presented for each level.

The measured OH reactivity, OHRecycling, and OHRreactants have similar trends from low altitude to high altitude – they decrease to values less than $1\,s^{-1}$ at the highest altitudes. However, in the $0\sim2$ km layer, the median measured OH reactivity ($4.0\pm1.0\,s^{-1}$) is greater than the median OHRecycling ($3.3\pm0.8\,s^{-1}$), and even greater than the median OHReactants ($1.6\pm0.4\,s^{-1}$). The uncertainty of OHRecycling is calculated based on the uncertainties of measured HO_2/OH ratio and the OH concentration. The uncertainty of OHReactants is based on the uncertainties of all measured OH reactants and their reaction coefficients with OH. The differences between OHReactans and the other two methods are statistically significant because the OHReactants falls out of the observation uncertainties range in the lowest layer. If the wall loss is 2.5–$2.9\,s^{-1}$ as suggested by laboratory tests, then the measured OH reactivity and OHRcycling would agree, although the difference between with the measured OH reactivity and OHReactant would still be significant. The measured OH reactivity is also greater than both OHRecycling and OHReactants above 2 km.

To verify this conclusion, a two-sample t-test is conducted between the OHReactant and OHRrecycling and the results show that these two variables are significantly different with the 99% confidence interval. The significance is also proved between the measured OH reactivity and OHReactant. The difference between the measured OH reactivity and OHRreactants suggests the presence of unknown OH reactants in the boundary layer that can affect the OH reactivity up to 4 km
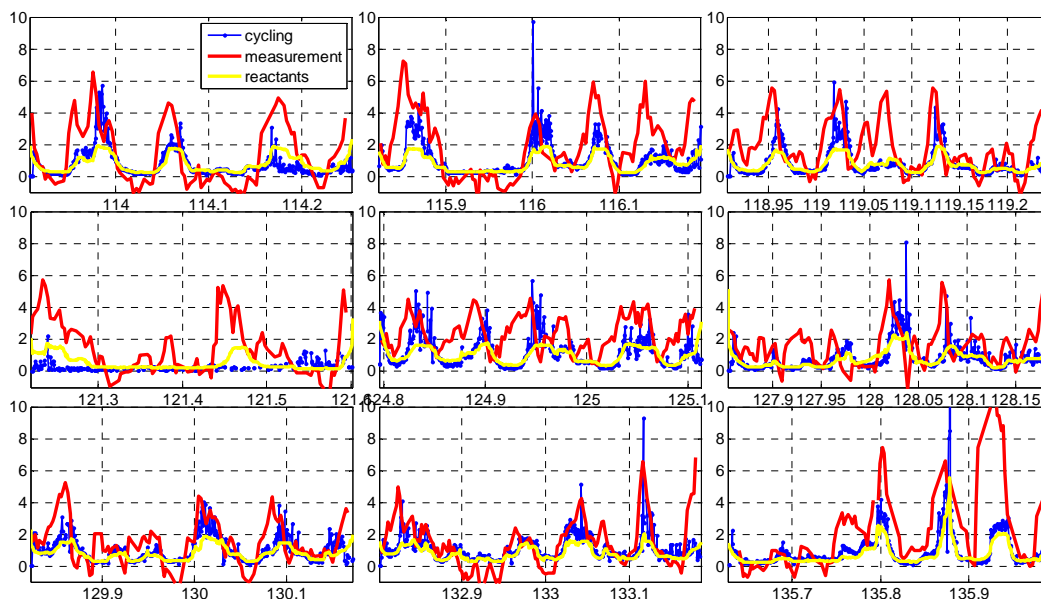
Fig. 6. OH reactivity measurement during the second phase of INTEX-B. Each panel is for one single flight. In each panel, the X-axis is Julian day and the Y-axis is the three types of OH reactivity discussed in the text, the measured OH reactivity (red), the calculated OH reactivity based on cycling (blue) and the calculated OH reactivity based on all measured reactants (yellow). The measured OH reactivity has been smoothed with a 3-point running average.
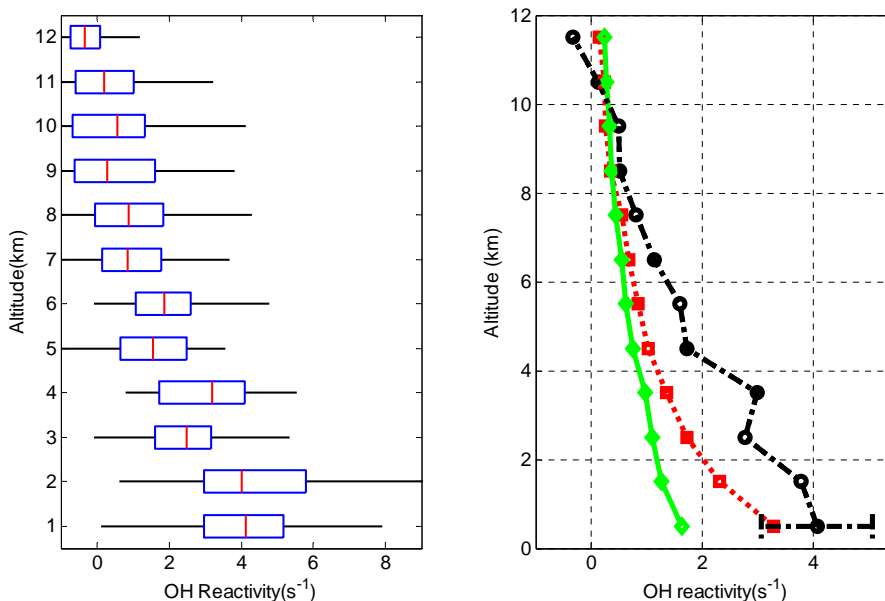

Fig. 7. Measured OH reactivity (left) and the comparison (right) of the three types of OH reactivity through the troposphere during the second phase of INTEX-B field campaign. In the left panel, the two ends of the box show the lower quartile, and upper quartile values. The line inside the box shows the median value. The lines extending from each end of the box shows the extent of the rest of the data (1.5 times the interquartile range). In the right panel, the black dash-dotted line with circles is the median measured OH reactivity, the red dotted line with squares is the median OHRrecycling, and the green solid line with diamonds is the median OHRreactants. The horizontal bar indicates the uncertainties (2σ) of the observations.
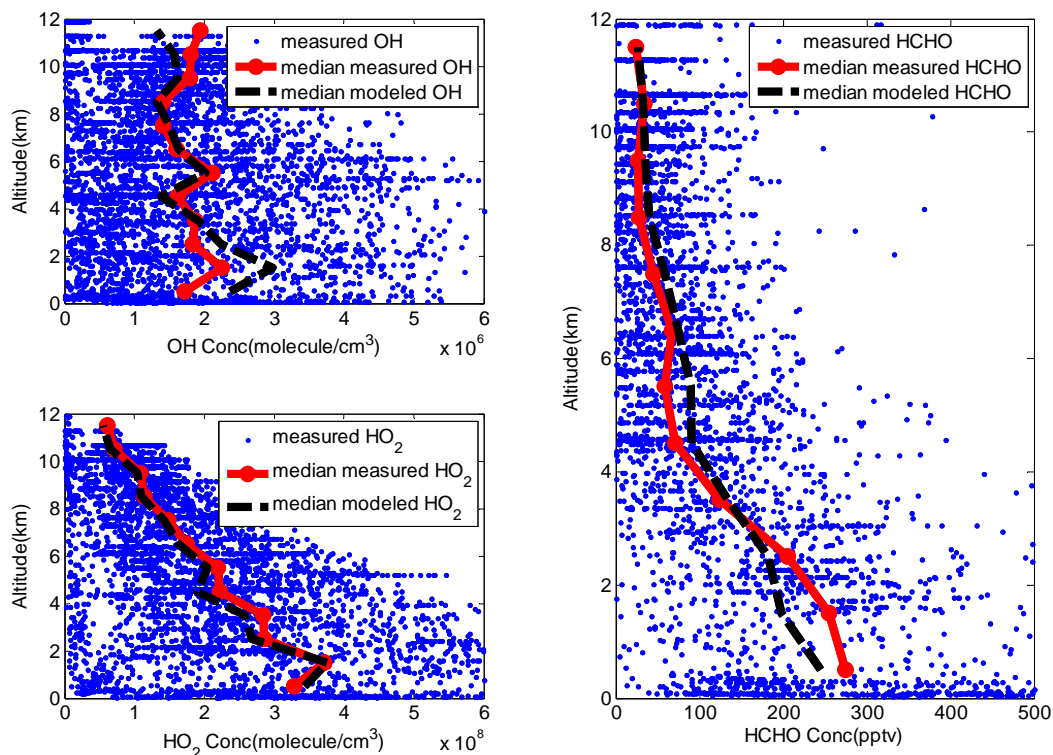
Fig. 8. Comparison of median altitude profiles for measured and modeled OH, HO$_2$ and HCHO during the second phase of INTEX-B. The median measurements are shown as a solid line with circles and the median model calculations are shown as a dashed line. Individual INTEX-B 1-min measurements are also presented (blue dots).

or so. This difference also suggests that about half of the OH reactivity is missing at these lower altitudes. Although the difference between the measured OH reactivity and OHRreactants extends higher than 2 km, it becomes less and statistically insignificant.

Some unmeasured oxidation products of hydrocarbons and other atmospheric constituents can react with OH. These were not in the list of atmospheric constituents used to calculate OHReactants. Quite a few intermediate and end products, including HCHO, H$_2$O$_2$, CH$_3$OOH, acetaldehyde, propanal, methanol, ethanol, acetone, have been measured and constrained in the box model. Therefore the oxidation products generated in the model other than these species have fairly small contribution to OH reactivity considering the low VOC level. These intermediate reaction products cannot account for the missing OH reactivity.

The differences between the measured OH reactivity and OHRreactants should be reflected in the differences between measured and modeled OH because the modeled OH uses the same OH reactants and reaction rate coefficients as OHRreactants. A chemical box model is used by NASA Langley Research Center to calculate the OH and HO$_2$ (called "LaRC" model" in this paper). The model detail is described elsewhere (Crawford et al., 1999; Olson et al., 2004). The model
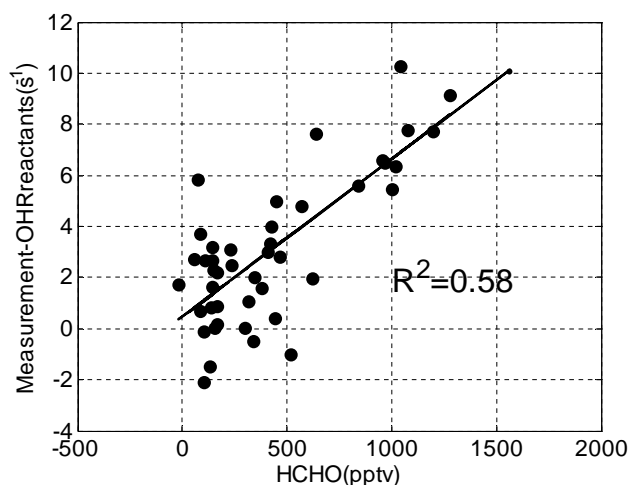

Fig. 9. Dependence of difference between OH reactivity measurement and OHRreactants on HCHO below 2 km and when NO is below 100 pptv.

is constrained by the observations of O$_3$, CO, NO$_2$, NO, NMHC, acetone, methanol, dew point, temperature, pressure, and photolysis frequencies. Diurnal steady-state means

that the model is run repeatedly over an entire day using the observed conditions until the concentrations of longer lived species like H_2O_2 do not change for any given time of day. The advantage of this method is to ensure the long-lived species are eventually in balance with other species.

Figure 8 presents the vertical profile of measured and modeled OH, HO_2 and HCHO during the second phase of INTEX-B. The measured and modeled OH and HO_2 disagree the most below 2 km altitude and then gradually come into agreement above 4 km altitude (Fig. 8). Below 2 km, the model calculation of OH is about 30% higher than the measurement. Meanwhile, the model calculation of HO_2 agrees very well with the measurement. Since OH and HO_2 were measured simultaneously in ATHOS instrument (Faloona et al., 2004), this difference is unlikely from absolute instrument artifacts only. If OH reactivity were missing from the model below 2 km, as Fig. 8 suggests, then there would be less OH loss in the model because the model uses only the measured atmospheric species. These are the same reactants with OH that go into the OHRreactants. This observation of missing OH reactivity is consistent with the over-predicted OH.

As an intermediate product from VOC oxidation, formaldehyde (HCHO) is a good indicator for hydrocarbon photochemistry because it is a product of oxidation of hydrocarbons by OH. Moreover, HCHO is not constrained in the LaRC model simulation. It is worthwhile to compare the modeled and measured HCHO. This comparison will test the understanding of the photochemistry using the measurement of another atmospheric constituent from an independent instrument. As shown in Fig. 8, the most under-predicted HCHO appears at altitudes from the surface to 2 km height. Could this extra amount of HCHO be from some atmospheric constituents that contribute to the missing OH reactivity? Could this missing OH reactivity come from highly reactive VOCs, or some other sulfuric, halogenated species? From the analysis of individual flights, we have noticed that the difference between measurement and OHRreactants appears when HCHO reaches a peak. As shown in Fig. 9, the difference between the OH reactivity measurement and OHRreactants is correlated with HCHO concentration below 2 km when NO is below 100 pptv, with a correlation coefficient R^2=0.58. This correlation indicates indirectly that the missing OH reactivity could be from some highly reactive VOCs that have HCHO as a product of oxidation.

From all the analyses above, the over-predicted OH and under-predicted HCHO are consistent with the missing OH reactivity, which is the measured OH reactivity – OHRreactants. Since 1000 pptv HCHO contributes less than $0.2\,s^{-1}$ OH reactivity in the boundary layer, it is more likely that HCHO serves as an indicator instead of contributing a big part to the missing OH reactivity. On the other hand, if we assume the missing OH reactivity is from some other oxygenated VOCs and we increase the current acetaldehyde concentration by a factor of 10 in the boundary layer, model calculations show that the total OH reactivity increases by 40%, OH decreases 65%, HCHO increases 65% and HO_2 decreases 15%. HO_2 is less sensitive than OH and HCHO in the model responding to the extra acetaldehyde. Qualitatively these model outputs agree well with the over-predicted OH and under-predicted HCHO for the missing OH reactivity. This result will shed some light on finding the missing species and thus reconciling the model and measurements.

4 Summary

A new airborne version of OH reactivity instrument was developed and tested on the NASA DC-8 aircraft. OH reactivity was successfully measured for the first time above Earth's surface during the second phase of the INTEX-B aircraft mission. The in situ and laboratory calibrations indicate good response of this new instrument under different pressure conditions. For INTEX-B Phase II, which was conducted mainly over Pacific Ocean, the OH reactivity measurements, the OH reactivity calculated with the measured OH reactants, and the OH reactivity calculated from OH steady-state all show the trend of OH reactivity decreasing with altitude. However, a difference between the measurements and calculations exists at altitudes below 4 km and is most pronounced in the 0~2 km layer. The measured OH reactivity ($4.0\pm1.0\,s^{-1}$) is larger than the calculated OH reactivity from cycling ($3.3\pm0.8\,s^{-1}$), and even larger than the calculated OH reactivity from the total measurements of all OH reactants ($1.6\pm0.4\,s^{-1}$). Model calculation shows the missing OH reactivity is qualitatively consistent with the over-predicted OH and under-predicted HCHO in the 0~2 km layer. The missing OH reactivity is correlated with HCHO in this layer, suggesting that it is most likely related to some highly reactive VOCs that are missing in the measurements and have HCHO as a product of oxidation. The missing OH reactivity in the boundary layer indicates the shorter OH lifetime, and thus implies the longer lifetimes for CH_4, CO and NO_2 than in current models. Future assessments of atmospheric reactivity should be made by measurement rather than either of the calculated methods performed here

Edited by: S. Madronich

References

Atkinson, R., Baulch, D. L., Cox, R. A., Crowley, J. N., Hampson, R. F., Hynes, R. G., Jenkin, M. E., Rossi, M. J., Troe, J., and IUPAC Subcommittee: Evaluated kinetic and photochemical data for atmospheric chemistry: Volume II - gas phase reactions of organic species, Atmos. Chem. Phys., 6, 3625–4055, 2006, http://www.atmos-chem-phys.net/6/3625/2006/.

Atkinson, R., Baulch, D. L., Cox, R. A., Crowley, J. N., Hampson, R. F., Hynes, R. G., Jenkin, M. E., Rossi, M. J., and Troe, J.: Evaluated kinetic and photochemical data for atmospheric chemistry: Volume III - gas phase reactions of inorganic halogens, Atmos. Chem. Phys., 7, 981–1191, 2007, http://www.atmos-chem-phys.net/7/981/2007/.

Crawford, J., Davis, D., Olson, J., Chen, G., Liu, S., Gregory, G., Barrick, J., Sachse, G., Sandholm, S., Heikes, B., Singh, H., and Blake, D.: Assessment of upper tropospheric HO_x sources over the tropical Pacific based on NASA GTE/PEM data: Net effect on HO_x and other photochemical parameters, J. Geophys. Res.-Atmos., 104, 16 255–16 273, 1999.

Di Carlo, P., Brune, W. H., Martinez, M., Harder, H., Lesher, R., Ren, X. R., Thornberry, T., Carroll, M. A., Young, V., Shepson, P. B., Riemer, D., Apel, E., and Campbell, C.: Missing OH reactivity in a forest: Evidence for unknown reactive biogenic VOCs, Science, 304, 722–725, 2004.

Dubey, M. K., Hanisco, T. F., Wennberg, P. O., and Anderson, J. G.: Monitoring potential photochemical interference in laser-induced fluorescence measurements of atmospheric OH, Geophys. Res. Lett., 23, 3215–3218, 1996.

Faloona, I. C., Tan, D., Lesher, R. L., Hazen, N. L., Frame, C. L., Simpas, J. B., Harder, H., Martinez, M., Di Carlo, P., Ren, X. R., and Brune, W. H.: A laser-induced fluorescence instrument for detecting tropospheric OH and HO2: Characteristics and calibration, J. Atmos. Chem., 47, 139–167, 2004.

Jeanneret, F., Kirchner, F., Clappier, A., van den Bergh, H., and Calpini, B.: Total VOC reactivity in the planetary boundary layer 1. Estimation by a pump and probe OH experiment, J. Geophys. Res.-Atmos., 106, 3083–3093, 2001.

Kovacs, T. A. and Brune, W. H.: Total OH loss rate measurement, J. Atmos. Chem., 39, 105–122, 2001.

Kovacs, T. A., Brune, W. H., Harder, H., Martinez, M., Simpas, J. B., Frost, G. J., Williams, E., Jobson, T., Stroud, C., Young, V., Fried, A., and Wert, B.: Direct measurements of urban OH reactivity during Nashville SOS in summer 1999, J. Environ. Monitor., 5, 68–74, 2003.

Olson, J. R., Crawford, J. H., Chen, G., Fried, A., Evans, M. J., Jordan, C. E., Sandholm, S. T., Davis, D. D., Anderson, B. E., Avery, M. A., Barrick, J. D., Blake, D. R., Brune, W. H., Eisele, F. L., Flocke, F., Harder, H., Jacob, D. J., Kondo, Y., Lefer, B. L., Martinez, M., Mauldin, R. L., Sachse, G. W., Shetter, R. E., Singh, H. B., Talbot, R. W., and Tan, D.: Testing fast photochemical theory during TRACE-P based on measurements of OH, HO2, and CH2O, J. Geophys. Res.-Atmos., 109(16), D15S10, doi:10.1029/2003jd004278, 2004.

Ren, X. R., Harder, H., Martinez, M., Lesher, R. L., Oliger, A., Shirley, T., Adams, J., Simpas, J. B., and Brune, W. H.: HOx concentrations and OH reactivity observations in New York City during PMTACS-NY2001, Atmos. Environ., 37, 3627–3637, 2003.

Ren, X. R., Harder, H., Martinez, M., Faloona, I. C., Tan, D., Lesher, R. L., Di Carlo, P., Simpas, J. B., and Brune, W. H.: Interference testing for atmospheric HOx measurements by laser-induced fluorescence, J. Atmos. Chem., 47, 169–190, 2004.

Ren, X. R., Brune, W. H., Oliger, A., Metcalf, A. R., Simpas, J. B., Shirley, T., Schwab, J. J., Bai, C. H., Roychowdhury, U., Li, Y. Q., Cai, C. X., Demerjian, K. L., He, Y., Zhou, X. L., Gao, H. L., and Hou, J.: OH, HO2, and OH reactivity during the PMTACS-NY Whiteface Mountain 2002 campaign: Observations and model comparison, J. Geophys. Res.-Atmos., 111(12), D10S03, doi:10.1029/2005JD006126, 2006.

Sadanaga, Y., Yoshino, A., Watanabe, K., Yoshioka, A., Wakazono, Y., Kanaya, Y., and Kajii, Y.: Development of a measurement system of OH reactivity in the atmosphere by using a laser-induced pump and probe technique, Rev. Sci. Instrum., 75, 2648–2655, 2004.

Sadanaga, Y., Yoshino, A., Kato, S., and Kajii, Y.: Measurements of OH reactivity and photochemical ozone production in the urban atmosphere, Environ. Sci. Technol., 39, 8847–8852, 2005.

Sander, S. P., Friedl, R. R., Ravishankara, A. R., Golden, D. M., Kurylo, M. J., Molina, M. J., Moortgat, G. K., Keller-Rudek, H., Finlayson-Pitts, B. J., Wine, P. H., Huie, R. E., and Orkin, V. L.: Chemical Kinetics and Photochemical Data for Use in Atmospheric Studies Evaluation Number 15, 2006.

Shirley, T. R., Brune, W. H., Ren, X., Mao, J., Lesher, R., Cardenas, B., Volkamer, R., Molina, L. T., Molina, M. J., Lamb, B., Velasco, E., Jobson, T., and Alexander, M.: Atmospheric oxidation in the Mexico City Metropolitan Area (MCMA) during April 2003, Atmos. Chem. Phys., 6, 2753–2765, 2006, http://www.atmos-chem-phys.net/6/2753/2006/.

Singh, H. B., Brune, W. H., Crawford, J. H., Flocke, F., and Jacob, D. J.: Chemistry and transport of pollution over the Gulf of Mexico and the Pacific: Spring 2006 INTEX-B Campaign overview and first results, Atmos. Chem. Phys. Discuss., 9, 363–409, 2009, http://www.atmos-chem-phys-discuss.net/9/363/2009/.

Sinha, V., Williams, J., Crowley, J. N., and Lelieveld, J.: The Comparative Reactivity Method - a new tool to measure total OH Reactivity in ambient air, Atmos. Chem. Phys., 8, 2213–2227, 2008, http://www.atmos-chem-phys.net/8/2213/2008/.

Sommariva, R., Bloss, W. J., Brough, N., Carslaw, N., Flynn, M., Haggerstone, A.-L., Heard, D. E., Hopkins, J. R., Lee, J. D., Lewis, A. C., McFiggans, G., Monks, P. S., Penkett, S. A., Pilling, M. J., Plane, J. M. C., Read, K. A., Saiz-Lopez, A., Rickard, A. R., and Williams, P. I.: OH and HO2 chemistry during NAMBLEX: roles of oxygenates, halogen oxides and heterogeneous uptake, Atmos. Chem. Phys., 6, 1135–1153, 2006, http://www.atmos-chem-phys.net/6/1135/2006/.

Tan, D., Faloona, I., Simpas, J. B., Brune, W., Olson, J., Crawford, J., Avery, M., Sachse, G., Vay, S., Sandholm, S., Guan, H. W., Vaughn, T., Mastromarino, J., Heikes, B., Snow, J., Podolske, J., and Singh, H.: OH and HO2 in the tropical Pacific: Results from PEM-Tropics B, J. Geophys. Res.-Atmos., 106, 32 667–32 681, 2001.